Plant Cell Physiol. 59(11): 2350–2365 (2018)
doi:10.1093/pcp/pcy157

Running head: Polyprenols influence plastid membrane dynamics

Article title: Medium-Chain Polyprenols Influence Chloroplast Membrane Dynamics In *Solanum Lycopersicum*.

Authors: Kristen Van Gelder[a1], Kevin A. Rea[a1], Lilia K.A. Virta[a1], Kenna L. Whitnell[1], Michael Osborn[1], Maritza Vatta[1], Alexandra Khozin[1], Karolina Skorupinska-Tudek[2], Liliana Surmacz[2], Tariq A. Akhtar[1*]

Author addresses:
[1] Department of Molecular and Cellular Biology, University of Guelph, Guelph, ON, N1G 2W1, Canada.
[2] Institute of Biochemistry and Biophysics, Polish Academy of Sciences, Pawinskiego 5a, 02-106 Warsaw, Poland.

[a] These authors contributed equally

*Corresponding author
Tariq A. Akhtar
Department of Molecular and Cellular Biology,
University of Guelph, Guelph, ON, N1G 2W1, Canada
Phone: (519) 824-4120 ext. 54794
Fax: (519) 837-1802
Email: takhtar@uoguelph.ca

Abbreviations:
Arabidopsis cis-prenyltransferase 7 (AtCPT7)
carboxypeptidase Y (CPY)
cis-prenyltransferases (CPTs)
2,6-dichlorophenolindophenol (DCPIP)
differential scanning calorimetry (DSC)
dimethylallyl pyrophosphate (DMAPP)
farnesyl diphosphate (FPP)
five-carbon (C5)
geranyl diphosphate (GPP)
geranylgeranyl diphosphate (GGPP)
isopentenyl pyrophosphate (IPP)
lavandulyl diphosphate synthase (LPPS)
mevalonic acid (MVA)
methylerythritol phosphate (MEP)
neryl diphosphate (NPP)
photosynthetic photon flux density (PPFD)
Solanum lycopersicum cis-prenyltransferase 5 (SlCPT5)
trans-prenyltransferases (TPTs)

ABSTRACT

The widespread occurrence of polyprenols throughout the plant kingdom is well documented, yet their functional role is poorly understood. These lipophilic compounds are known to be assembled from isoprenoid precursors by a class of enzymes designated as *cis*prenyltransferases (CPTs), which are encoded by small CPT gene families in plants. In this study, we report that RNAi-mediated knockdown of one member of the tomato CPT family (SlCPT5) reduced polyprenols in leaves by ~70%. Assays with recombinant SlCPT5 produced in *E. coli* determined that the enzyme synthesizes polyprenols of approximately 50-55 carbons (Pren-10, Pren-11) in length and accommodates a variety of *trans*-prenyldiphosphate precursors as substrates. Introduction of SlCPT5 into the polyprenol-deficient yeast *Δrer2* mutant resulted in the accumulation of Pren-11 in yeast cells, restored proper protein *N*glycosylation, and rescued the temperature sensitive growth phenotype that is associated with its polyprenol deficiency. Subcellular fractionation studies together with *in vivo* localization of SlCPT5 fluorescent protein fusions demonstrated that SlCPT5 resides in the chloroplast stroma and that its enzymatic products accumulate into both thylakoid and envelope membranes. Transmission electron microscopy images of polyprenol-deficient leaves revealed alterations in chloroplast ultrastructure and anisotropy measurements revealed a more disordered state of their envelope membranes. In polyprenol-deficient leaves, CO2 assimilation was hindered and their thylakoid membranes exhibited lower phase transition temperatures and calorimetric enthalpies, which coincided with a decreased photosynthetic electron transport rate. Taken together, these results uncover a role for polyprenols in governing chloroplast membrane dynamics.

KEYWORDS:

Polyprenol, cis-prenyltransferase, Solanum lycopersicum, membrane fluidity, photosynthesis, chloroplast envelope

INTRODUCTION

Plant isoprenoids constitute one of the most abundant classes of natural products (Reviewed by Kirby and Keasling 2009). These compounds serve as pre-cursors and/or cofactors in a variety of essential processes such as energy capture and conversion (carotenoids, chlorophylls and tocopherols), electron transport (phylloquinone, plastoquinone and ubiquinone), membrane architecture and assembly (sterols), and in hormone-mediated patterns of plant development (abscisic acid, brassinosteroids, cytokinins, gibberellins, and strigolactones). Isoprenoids, such as terpenes, also provide the first line of defense during plantpathogen interactions and play a central role in attracting pollinators during the plant reproductive stage (Tholl and Lee 2011). Despite the fact that this diverse set of compounds has been historically well-studied, there is one particular class of plant isoprenoids which have largely been ignored – the polyisoprenoids. This subset of isoprenoids was first identified in cellulose pulp extracts over 50 years ago (Lindgren 1965) and these compounds have since been shown to occur throughout the plant kingdom (Swiezewska and Danikiewicz 2005; Skorupinska-Tudek et al. 2008), yet questions about their biosynthesis, compartmentation and physiological function still remain.

Plant polyisoprenoids are hydrophobic polymers that are composed of the universal fivecarbon (C5) isoprenoid precursors, isopentenyl pyrophosphate (IPP) and its isomer dimethylallyl pyrophosphate (DMAPP). These C5 'building blocks' are produced in plants via two spatially separated pathways: the mevalonic acid (MVA) pathway in the cytosol and the methylerythritol phosphate (MEP) pathway in the plastid. Biosynthesis of polyisoprenoids is believed to occur in two stages. First, DMAPP and a variable number of IPP units are condensed in a head-to-tail orientation by *trans*-prenyltransferases (TPTs) to produce a *trans*-oligoprenyl intermediate composed of two (geranyl diphosphate, GPP), three (farnesyl diphosphate, FPP) or four (geranylgeranyl diphosphate, GGPP) C5 units. TPTs are present in both cell compartments and synthesize GPP and GGPP from precursors derived from the plastidial MEP pathway, while FPP synthesis occurs in the cytosol via the MVA pathway (Rohmer 1999; Rodríguez- Conceptión and Boronat 2002). Next, these *trans*-prenyl diphosphate initiators are then extended with a variable number of IPP units by a distinct group of enzymes known as *cis*prenyltransferases (CPTs) to produce polyisoprenoids that range in length from C10 to over several hundred isoprene units (Swiezewska and Danikiewicz 2005). One member of the tomato CPT family, neryldiphosphate synthase (NDPS1/SlCPT1) is an exception in that it condenses IPP and DMAPP into the *cis*-isomer of GPP, known as neryldiphosphate (Schilmiller et al. 2009). The diversity in size of plant polyisoprenoids is achieved by the activity of specific CPTs, which are encoded by small families (3 to 9 members) in the genomes of all plants (Akhtar et al. 2013). The enzymatic products of these particular CPTs are accordingly designated as short- (C10-C35), medium- (C40-C70), or long-chain (C75 and beyond) polyisoprenoids based on their size (Schulbach et al. 2000; Kharel et al. 2006; Surmacz and Swiezewska 2011). However, assigning a particular class of polyisoprenoids to the activity of a single CPT is often complicated by the co-occurrence of all classes of polyisoprenoids in the same tissue or cell-type and the overlapping expression patterns of the CPTs that are thought to be responsible for their synthesis (Surmacz and Swiezewska 2011; Kera et al. 2012; Akhtar et al. 2013).

Polyisoprenoids exist mainly as free alcohols (and to a lesser extent as esters with carboxylic acids or phosphates) and are divided into two groups: the dolichols and polyprenols. Plant dolichols typically contain 15-17 C5 units (Dol-15 to Dol-17; C75-C85) and are fully saturated at their terminal (α-isoprene) unit while polyprenols are α-unsaturated and the range of their chain-length is far more diverse; polyprenols in numerous plants contain 6 to 12 C5 units

(Pren-6 to Pren-12; C30-C60). Dolichols are most notably known for their indispensable role in protein *N*glycosylation whereby a 'glycan', composed of 14 monosaccharide molecules, is assembled onto an endoplasmic reticulum membrane-bound dolichol molecule prior to being transferred to nascent polypeptides that enter the secretory pathway. The functional role of plant polyprenols is somewhat more enigmatic and is complicated by the fact that almost nothing is known about where these compounds reside within the cell and which particular CPTs are involved in their synthesis. What is clear is that virtually all plant leaves and other green tissues appear to accumulate polyprenols between 45 and 55 carbons in length (C45-C55, Pren-9 to Pren-11), suggesting that these 'medium-chain' polyprenols may serve more of an evolutionarily conserved purpose than previously thought (Chojnacki and Vogtman 1984; Swiezewska and Chojnacki 1988; Swiezewska et al. 1994; Kurisaki et al. 1997; Sakaihara et al. 2000).

Based solely on *in vitro* studies with model membranes, it has been suggested that polyprenols, by virtue of their hydrophobicity and tendency to accumulate into bio-membranes, act as modulators of membrane dynamics (Zhou and Troy 2003; Hartley and Imperiali 2012).Until recently, however, *in vivo* evidence to support these conclusions was lacking. Studies by Akhtar et al. (2017) identified a CPT from *Arabidopsis thaliana* (AtCPT7) which synthesizes polyprenols between 45 and 55 carbons in length which accumulate in chloroplast membranes and in their absence results in impaired photosynthetic function. Here we report the identification of an orthologous CPT in *Solanum lycopersicum* (cultivated tomato) and present evidence that polyisoprenoids serve a more general role in governing overall chloroplast membrane dynamics.

RESULTS

RNAi mediated knockdown of SlCPT5

The *S. lycopersicum* genome encodes a seven-member family of CPTs that are believed to be involved in the synthesis of polyisoprenoids. To date, only three members (SlCPT1/NDPS1, SlCPT2 and SlCPT3) of this family have been functionally characterized in any detail (Schilmiller et al. 2009; Akhtar et al. 2013; Brasher et al. 2015; Matsuba et al. 2015) and it is unclear which remaining member(s) of the tomato CPT family are responsible for the synthesis of medium chain polyprenols (C45-C55, Pren-9 to Pren-11). We posited that SlCPT5 could be the enzyme that synthesizes these compounds based on the following lines of evidence: First, SlCPT5 is expressed at high levels in tomato leaf tissue, which is the main site of synthesis and accumulation of polyprenols (Brasher et al. 2015), whereas the other members of the SlCPT family are not (Akhtar et al. 2013). Second, *in vitro* assays with recombinant SlCPT5 indicate that the enzyme synthesizes medium-chain polyprenols of approximately 55 carbons in length (Akhtar et al. 2013). It is important to note that SlCPT4 also synthesizes medium-chain polyprenols, *in vitro*, however it is expressed at levels that are an order of magnitude below those of SlCPT5. Third, SlCPT5 is closely related to the recently characterized AtCPT7 that is responsible for the synthesis of these same compounds in *Arabidopsis* (Brasher et al. 2015; Akhtar et al. 2017). Lastly, *in silico* evidence points to a robust up-regulation of SlCPT5 during oxidative stress (Fei et al. 2011) which is also known to trigger the accumulation of leaf polyprenols in a variety of plant species (Swiezewska and Danikiewicz 2005; Bajda et al. 2009). We therefore performed RNAi-mediated knockdown of SlCPT5 and monitored SlCPT5 expression and polyprenol abundance in the leaves from nine independent transformants. This analysis revealed an ~85% decrease in SlCPT5 mRNA abundance and virtually undetectable levels of the mature

protein in three out of the nine independent RNAi-lines (Fig. 1A). In these transformants, the expression levels of SlCPT4, which has 80% identity with SlCPT5 at the nucleotide level (Akhtar et al. 2013), was unaffected (Fig. S1). Under standard growth conditions, we did not observe any visible phenotypes between wild type plants and these independent RNAi lines. The main polyprenols that are present in tomato leaves are those containing 45 to 55 carbons (Pren-9 to Pren-11; Fig. 1B) and, relative to wild type, the leaf polyprenol content in the three SlCPT5 RNAi lines was reduced by an average of 64% (Fig. 1C). The level of dolichols in these RNAi lines, which range in size from 75-85 carbons in length (Dol-15 to Dol-17), were consistent with what is normally found in wild type tomato leaves (Fig. 1C). Among the nine independent transgenic RNAi lines that were generated, one particular Line (RNAi-17) was identified in which SlCPT5 mRNA abundance was unchanged and polyisoprenoid analysis of this line indicated that its leaves accumulate wild type levels of polyprenols and dolichols (Fig. S2). Together, these results point to a role for SlCPT5 in medium-chain polyprenol biosynthesis.

Functional complementation of the dolichol deficient *Δrer2* yeast mutant by SlCPT5

To further examine the involvement of SlCPT5 in polyprenol biosynthesis, complementation tests were performed in the yeast *Δrer2* mutant. This mutant cannot synthesize dolichol and is therefore impaired in protein *N*-glycosylation which halts growth at elevated temperatures (Sato et al. 1999). Interestingly, medium-chain polyprenols can functionally substitute for dolichols in this yeast strain and restore growth of the mutant at nonpermissive temperatures (Rush et al. 2010). Introduction of the mature version of SlCPT5 (*sans* the predicted transit peptide) into the *Δrer2* mutant rescued its growth at 37°C, as did the native RER2 gene when either gene was expressed under the control of the native RER2 promoter; introduction of the expression vector alone did not (Fig. 2A). Polyisoprenoid analysis of these strains revealed that the *Δrer2* mutant cells expressing SlCPT5 accumulated a family of medium chain dolichols of 50-60 carbons (Dol-10 to Dol-12) in length while the cells expressing the native RER2 gene accumulated dolichols of 75-85 carbons (Dol-15 to Dol-17) in length (Fig. 2B). We next assayed the glycosylation status of the prototypical glycoprotein, carboxypeptidase Y (CPY), in the *Δrer2* mutant strains described above to determine whether the rescue of *Δrer2* mutant growth and their subsequent accumulation of medium-chain dolichols upon introduction of SlCPT5 resulted from the restoration of the *N*-glycosylation pathway. Mutant cells harboring the vector alone accumulated hypo-glycosylated forms of CPY that were missing between one and four *N*-linked glycans, whereas cells expressing SlCPT5 or the native RER2 protein only contained the mature fully glycosylated form of CPY (Fig. 2C). These results therefore suggest that medium-chain dolichols are sufficient to rescue the growth defects and restore proper *N*-glycosylation in the yeast *Δrer2* mutant and that SlCPT5 functions in their biosynthesis, *in vivo*.

Recombinant SlCPT5 enzyme characterization and identification of catalytically essential amino acid residues

To directly assay for SlCPT5 *cis*-prenyltransferase enzyme activity, the open reading frame of the mature protein, minus the predicted *N*-terminal transit peptide, was first introduced into *E. coli* as a fusion protein with a *C*-terminal hexahistidine tag. The recombinant protein was subsequently purified to apparent homogeneity by Ni2+-affinity chromatography, as determined by SDS-PAGE and immunoblot analysis with a peptide-specific antibody raised against SlCPT5 (Fig. 3A). Next, *in vitro* enzyme assays were conducted by providing the recombinant protein with one of four prenyl initiator substrates (GPP, NPP, FPP, or GGPP)

together with 14C-IPP. The enzymatic polyprenyl diphosphate products were acid-hydrolyzed to their corresponding alcohols and then resolved by reverse phase thin-layer chromatography to determine their relative sizes. This analysis demonstrated that recombinant SlCPT5 could extend the length of any of these substrates to approximately 55 carbons (Fig. 3B). However, steady-state kinetic analysis revealed that the enzyme had an approximately seven-fold higher preference for FPP and GGPP, compared to GPP. Neryl diphosphate (NPP), the *cis*-isomer of GPP which accumulates to relatively high levels in tomato leaves (Schilmiller et al. 2009), also proved to be an inefficient substrate for SlCPT5 (Table 1). Densitometry analysis of the radiolabeled enzymatic products (following their separation on TLC plates) from assays with the various *trans*-prenyl co-substrates indicated that the polyprenols which were derived from FPP and GGPP largely migrated to a zone on TLC plates whose *Rf* value corresponded to C45-C55 in size (Fig. 3B). In contrast, assays with NPP and GPP resulted in products with a less defined size profile and broadly spanned zones corresponding to C25-C55. To gain insight into the structural features of SlCPT5 that contribute towards substrate and product specificities, the mature protein was homology modeled to the crystal structure of lavandulyl diphosphate synthase (LPPS; PDB ID: 5hc6) from *Lavandula x intermedia* (Liu et al. 2016). The overall quality of the model was validated using PROCHECK and ERRAT (Fig. S3) and the predicted substrates GGPP and IPP as well the catalytically essential Mg2+ cation were docked using AutoDock Vina with binding affinities of 1.0, -5.2, and -1.4 kcal mol-1, respectively. According to the model (Fig. 3C), a conserved suite of residues that were previously implicated in substrate binding and/or catalysis for various bacterial CPTs (Kharel et al. 2001), surround the predicted active site of the enzyme (corresponding residues in SlCPT5: D89, F133, R259, R265). The carboxyl group on D89 has experimentally been shown to assist the migration of the Mg2+ cation from IPP to GGPP so as to facilitate pyrophosphate removal from the latter (Fujihashi et al. 2001; Chang et al. 2003; Guo et al. 2005), whereas the benzyl moiety of F133 stabilizes the hydrocarbon backbone of IPP and orientates C4 of IPP towards C1 of GGPP (Fig. 3C). The positively charged guanidinium groups of R259 and R265 are believed to bind the pyrophosphate moiety of IPP and further stabilize the co-substrate (Kharel et al., 2001). To verify that these residues in SlCPT5 are in fact essential for enzyme activity, site-directed mutagenesis was performed in which the conserved aspartate and phenylalanine were replaced with alanine residues (D89A and F133A) while the two arginines were changed to serines (R259S and R265S). These mutated versions of SlCPT5 were then introduced into the *Δrer2* mutant and serially diluted cultures were tested for growth in complementation assays. As previously demonstrated, both SlCPT5 and the native RER2 were able to restore growth of the *Δrer2* mutant cells, however the mutated versions of SlCPT5 were unable to complement the mutant at the non-permissive temperature (Fig. 3D), in spite of being expressed (Fig. 3E), thereby suggesting a conserved catalytic function for these amino acid residues among the CPT family of enzymes.

Subcellular localization of SlCPT5 and medium-chain polyprenols

SlCPT5 and its close homologs from other plant species encode proteins with predicted *N*-terminal targeting peptides that are thought to guide these CPTs to the mitochondria, plastid, or endomembrane system (Surmacz and Swiezewska 2011; Akhtar et al. 2013). To assess the subcellular location of SlCPT5, we first transiently introduced the full-length *SlCPT5* open reading frame as a *C*-terminal fusion with GFP into Arabidopsis protoplasts and tracked its subcellular residency via confocal microscopy. This analysis demonstrated that the fluorescent signal attributed to GFP completely overlapped with the chlorophyll

autofluorescence of the protoplasts (Fig. 4A). Next, tomato leaf plastids were fractionated into their corresponding subcompartments (envelope, stroma and thylakoids) and SlCPT5 accumulation was assessed by immunoblot analysis using peptide-specific antibodies. This analysis revealed that SlCPT5 resides exclusively in the stroma; the purity of each subcompartment was confirmed by the presence/absence of compartment-specific marker proteins and revealed that purified envelope, stroma and thylakoids were essentially uncontaminated by other fractions (Fig. 4B). Finally, we assayed each subcompartment of tomato leaf plastids for prenyltransferase enzyme activity and found that the majority was present in the stroma, coincident with the location of SlCPT5 (Fig. 4C). The hydrophobic polyprenol products that SlCPT5 synthesizes would not be predicted to reside in soluble stroma along with the enzyme, so we next analyzed the polyprenol contents of the various subcompartments of tomato plastids to determine the precise destination of these compounds. This analysis revealed that intact chloroplasts contained the same polyprenols (Pren-9 to Pren-11) that are encountered in leaf tissue and that these compounds largely accumulate into both the thylakoid and envelope subcompartments (Fig. 5A). Virtually no polyprenols were found in the stroma. When the total amount of Pren-9, Pren-10, and Pren-11 in these fractions were normalized to protein content, it was determined that the envelope contained approximately 2.5 fold more polyprenols in comparison to the thylakoid fraction (Fig. 5B). Strikingly, intact chloroplasts and their various subcompartments that were isolated from the SlCPT5 RNAi-lines contained ~65% less polyprenols (decreases of 57% in chloroplasts; 86% in envelope; and 50% in thylakoid fractions) when compared to wild type (Fig. 5B). Moreover, the prenyltransferase enzyme activity in the stroma was ~52% lower in the three RNAi lines (Supplemental Table S2). Low amounts of stromal polyprenols were observed in the RNAi lines and changed little in comparison to their wild type counterparts.

Polyprenol deficiency leads to impaired photosynthetic performance and altered plastidial membrane dynamics

To examine how the loss of medium-chain polyprenols affects the general ultrastructure of tomato chloroplasts, we compared transmission electron micrographs of chloroplasts from young tomato leaf tissue sections that were prepared from wild type leaves and those from two of the RNAi lines (RNAi-10 and RNAi-15). While the overall shape and size of chloroplasts from wild type and polyprenol-deficient leaves were similar, there was a noticeable change in the organization of the internal chloroplast membranes. Approximately 83% of the chloroplasts examined from the RNAi lines consisted of poorly stacked grana and longer stroma thylakoids (Fig. 6A). Additionally, the accumulation of plastoglobuli in these chloroplasts consistently outnumbered those observed from wild type leaves with an average of over 6 plastoglobuli per chloroplast in the RNAi lines compared to approximately 4 in wild type chloroplasts (Fig. S4). The accumulation of polyprenols in the plastidial membranes of tomato (Fig. 5B) prompted us to examine the consequences of polyprenol deficiency in both the envelope and thylakoid membranes. We first prepared chloroplast envelope membranes from the leaves of wild-type and the RNAi lines and then labelled them with the lipophilic fluorophore 1,6-diphenyl-1,3,5-hexatriene (DPH), which readily partitions into the lipid matrix of a wide variety of biomembranes (Shinitzky and Barenholz 1978). We then performed DPH fluorescence anisotropy measurements on these labelled envelope membranes. In theory, the degree of depolarization of DPH fluorescence emission (defined as fluorescence anisotropy, *r*) is determined by the rotational freedom of the fluorophore within the biomembrane it occupies (Lentz 1993). Any change in the steady-state fluorescence emitted by DPH is caused by an alteration of its lipid microenvironment and can therefore provide an

indirect measure of membrane order (Yamamoto et al. 1981; Ford and Barber 1983; Kunst et al. 1989; Dobrikova et al. 1997; Popova and Hincha 2007; Akhtar et al. 2017). It was determined that there was a significant decrease in the *r* value for DPH-labeled envelope membranes from the three independent RNAi lines relative to those observed from preparations of wild-type envelope membranes (Fig. 6B), indicating that the rotational freedom of DPH in polyprenol deficient membranes is enhanced as a result of an increasingly disordered or "fluid" state of the envelope. We next turned our attention to the thylakoids, which also accumulate significant amounts of polyprenols (Fig. 5B), and compared the integrity of thylakoid membranes from the leaves of wild type and the polyprenol-deficient RNAi lines via differential scanning calorimetry (DSC). This analysis permits detection of thermally induced conformational transitions of thylakoid membrane constituents (defined as the phase transition temperature, *T*m) and quantifies the enthalpy change (Δ*H*c) that is associated with the unfolding of thylakoid membrane proteins, thereby providing a measurement of thylakoid membrane protein stability (Smith and Low, 1989; Dobrikova et al. 2003; Krumova et al. 2010; Yang and Brouillette 2016). For these measurements, we focused on the RNAi-10 and RNAi-11 lines which showed the greatest degree of SlCPT5 mRNA knockdown and polyprenol reduction (Fig. 1). The calorimetric signals (thermogram) obtained from wild type thylakoids exhibited a sharp endothermic peak with an average *Tm* value of 94.6 ± 0.6°C and calorimetric enthalpies of 1961 ± 36 Joules g-1 (Fig. 6C). In comparison, thylakoids from the RNAi lines displayed thermograms with a noticeable shift towards lower enthalpies (1825 ± 76 Joules g-1) and phase transition temperatures (93.0 ± 0.9°C), suggesting that polyprenol-deficient thylakoid membranes and their constituents are destabilized relative to their wild type counterparts (Fig. 6C). Upon consecutive heating and cooling cycles, the sharp calorimetric signals obtained for thylakoid membranes disappeared, implying that the irreversible phase transitions observed were due to membrane protein denaturation/unfolding and not to the lipid constituents of these membranes. Considering the influence that polyprenol deficiency had on thylakoid membrane integrity, we next measured the rates of photosynthetic electron transport in thylakoids from wild type and the three independent RNAi lines using a spectrophotometric assay that monitors the reduction of the artificial electron acceptor, 2,6-dichlorophenolindophenol (DCPIP). DCPIP readily intercepts the passage of electrons from reduced plastoquinone to the cytochrome *b6f* complex, which is generally considered to be the rate-determining step in oxygenic photosynthesis (Govindjee and van Rensen, 1978; Heber et al. 1988; Hasan and Cramer, 2012). It was observed that polyprenol-deficient thylakoids exhibit an approximately 83% decrease in the rate of electron transport compared to their wild type counterparts (Fig. 6D). Since photosynthetic electron transport provides the reducing power necessary for carbon fixation, we next measured whether CO2 assimilation rates were affected by polyprenol deficiency as a function of photosynthetic photon flux density (PPFD). Under ambient levels of CO2 (400 ppm), photosynthetic CO2 assimilation rates at low PPFD differed little between fullyexpanded leaves from wild type and the three RNAi lines (Fig. 6E). However, at a moderate to high PPFD (above 400 µmol m-2 sec-1), CO2 assimilation rates were approximately 30% lower in leaves from the RNAi lines compared to their wild type counterparts (Fig. 6E). While it is well established that other plastidial isoprenoids also impact membrane dynamics (Havaux 1998; Gruszecki and Strzałka 2005), we found no significant differences in carotenoid or tocopherol levels between thylakoids and envelope membranes that were isolated from wild type and the polyprenol-deficient SlCPT5 RNAi lines (Table 2). In addition, the amount of chloroplast fatty acids and the degree of fatty acid saturation, both of which have been implicated in the

maintenance of chloroplast membrane architecture and integrity (McCourt et al. 1987; Hugly et al. 1989), were unchanged between wild type and the three independent RNAi lines (Fig. S5). Taken together, these results imply that polyprenol deficiency in tomato chloroplasts result in the destabilization of plastidial membranes which ultimately impairs photosynthetic performance.

DISCUSSION

Evidence for the occurrence of polyprenols in the green tissues of plants has been mounting for over 50 years (Lindgren 1965; Hemming 1983; Swiezewska et al. 1994). The results presented in this study confirm and extend these observations by demonstrating that polyprenols are synthesized within plastids by a CPT and that their accumulation into plastid membranes influences their membrane architecture and dynamics.

Using tomato (*S. lycopersicum*) as a model, we present biochemical and genetic evidence that one member of the tomato CPT gene family (SlCPT5) is involved in polyprenol biosynthesis. By targeting SlCPT5 for RNAi-mediated mRNA knockdown, we isolated three independent transgenic lines that were deficient in SlCPT5 expression and polyprenol accumulation. The enzymatic products of SlCPT5 were further confirmed *in vivo* by functional complementation of the yeast *Δrer2* mutant and *in vitro* by directly assaying the recombinantly produced enzyme. The medium-chain polyprenols of approximately 50 carbons in length (C50, Pren-10) that are produced by SlCPT5, together with its plastidial localization, fit well with previous reports that have described the accumulation of these compounds in the leaves of various plants and the corresponding CPT enzyme activity within chloroplasts (Daleo and Lezica 1977; Ravi et al. 1984; Kurisaki et al. 1997; Sakaihara et al. 2000; Akhtar et al. 2017). While recombinant SlCPT5 could accommodate a variety of *trans*-prenyl diphosphate substrates, *in vitro*, it is most likely that GGPP serves as its bona fide substrate *in planta* for the following reasons: First, recombinant SlCPT5 utilized only FPP and GGPP as substrates with kinetic constants that were reasonably consistent with previously characterized CPTs from bacteria and plants (Kharel et al. 2001; Schilmiller et al. 2009; Kera et al. 2012). Secondly, the plastidial localization of SlCPT5 places it in the same organelle where GGPP is mainly synthesized, while FPP is believed to be cytosolic in origin (Tholl and Lee 2011). Thirdly, structural characterization of Pren-10 from a variety of plants and most recently from *Arabidopsis* leaves (Swiezewska and Danikiewicz 2005; Akhtar et al. 2017) has shown that the molecule contains three internal *trans*-methyl groups and adopts a ω-*trans*3-*cis*6 configuration, which is consistent with a geranylgeranyl moiety linked to a tail of six isoprene units in a *cis* configuration.

The observation that SlCPT5 utilizes FPP and GGPP with similar efficiencies was fortuitous, in that it allowed us to exploit the yeast *Δrer2* mutant system in complementation assays. Yeast do not produce GGPP, but instead synthesize FPP as a precursor for dolichol and the *Δrer2* mutant is dolichol deficient due to the ablation of the CPT that is involved in its synthesis (Sato et al. 1999). The observation that the medium chain polyprenols produced by SlCPT5 can rescue the *Δrer2* mutant indicates that this mutant can convert shorter polyprenols (C45-C55) into dolichols by reducing their terminal isoprene unit and then substitute these ‘shortchain’ dolichols into their central *N*-glycosylation pathway. This implies that, at least in yeast, medium-chain polyprenols can serve as a scaffold within the ER membrane onto which the ‘glycan’ is assembled and must therefore adopt a similar place, orientation and conformation as dolichol. We return to this point below.

The yeast *Δrer2* mutant system also allowed us to test whether certain amino acid residues in SlCPT5 are catalytically essential. We chose to mutate four residues in SlCPT5 that are conserved amongst all other bacterial CPTs that have been characterized, which in SlCPT5 are D89, F133, R259, and R265. When these SlCPT5 variants were introduced into the yeast *Δrer2* mutant, none of the SlCPT5 mutants were able to rescue the *Δrer2* growth defect. Therefore, based on our modeling/mutagenesis data and those obtained from previous mutagenesis studies with bacterial CPTs, it appears that CPTs from bacteria and plants do indeed share a common enzymatic mechanism: Binding of GGPP results in a conformational change within the flexible loop that surrounds the allylic diphosphate binding site which stabilizes the enzyme substrate complex. Following stabilization, IPP binds and is coordinated by R259 and R265 via hydrogen bonding to the diphosphate group of IPP, while the associated Mg2+, coordinated by D89, is shuttled from IPP to GGPP and allows for the release of Mg2+ - pyrophosphate from GGPP. Additionally, F133 has dual functionality by both stabilizing and orientating the hydrocarbon moiety of IPP such that C4 of IPP and C1 of GGPP are proximal to one another. This close proximity allows attack of GGPP by IPP at C1 causing the release of GGPP's pyrophosphate, the formation of a new C-C bond, and a carbocation intermediate. In the final step of catalysis, proton abstraction of H2 from the carbocation occurs resulting in a new double bond in a *cis*-orientation. While GGPP exhibited an unfavourable binding affinity (1.0 kcal mol-1) in our homology model, it is important to note that the LPPS crystal structure to which SlCPT5 was modeled against is in apo form (Liu et al. 2016). Furthermore, the short α-helix and flanking loops that surround the allylic diphosphate binding site in various CPT crystal structures lack electron densities in this exact region (Chang et al. 2003; Liang 2009), which suggests that this region is highly flexible and may undergo conformational changes to stabilize the substrate in the allylic diphosphate binding site, as purported above.

To examine the effects of SlCPT5 knockdown in tomato plastids, we utilized two independent, yet complimentary biophysical approaches, to probe for changes in plastidial membrane dynamics that were brought about by the observed polyprenol deficiency in these lines. Firstly, DSC analysis revealed that polyprenol-deficient thylakoids consistently exhibited a downward shift in both the temperature and heat required to bring about calorimetric membrane phase transitions. These irreversible phase transitions that were typically observed are attributed to the thermal unfolding and denaturation of membrane proteins (Dobrikova et al. 2003; Krumova et al. 2010; Laczkó-Dobos et al. 2011), which occupy between 70 to 80% of the thylakoid membrane space (Kirchhoff et al. 2008). Therefore, it seems that the presence of polyprenols in thylakoids act to stabilize membrane protein constituents. While our analysis cannot specifically pinpoint which thylakoid proteins are disturbed by polyprenol deficiency, it appears that those involved in electron transport are particularly affected. The 83% decline in DCPIP reduction that was observed in our electron transport assays with polyprenol-deficient thylakoids suggest that polyprenols help facilitate the passage of the mobile plastoquinone electron carrier between the photosystem II and cytochrome *b6f* protein complexes. Whether polyprenols allosterically regulate or stabilize these membrane protein complexes by directly binding to them remains an open question. In this context, it is interesting to note that polyprenol-binding proteins have been identified in both bacteria and yeast (Albright et al. 1989; Datta and Lehrman 1993; Handa et al. 2005), so it is tempting to speculate that throughout the course of evolution plants have also maintained polyprenol recognition sequences in certain thylakoid membrane proteins to enable various aspects of polyprenol-mediated protein function.

It is also conceivable that polyprenols act as auxiliary stabilizers of membrane integrity through their interaction with the surrounding lipid acyl chain microenvironment. Our second approach to assess plastidial membrane integrity addressed this possibility by measuring the degree of DPH fluorescence polarization in polyprenol-deficient envelope membranes that were labeled with the lipophilic DPH fluorophore. These results clearly indicate that polyprenoldeficient envelope membranes adopt a more 'fluid' or disordered state, which suggests that polyprenols directly modulate fatty acyl chain mobility, as originally proposed by McCloskey and Troy (1980). Modeling studies predict that polyprenols adopt a 'chair-like' conformation, *in vivo*, which serves to compress their unusually long hydrophobic tail into a central coiled domain (Zhou and Troy 2003, Hartley and Imperiali 2012). In such a conformation, individual polyprenols would be ~22 Å from head to tail (about one-half the length of C55 in its extended form) and therefore be predicted to occupy only one leaflet of the envelope bilayer, with their coiled domain proximate to neighbouring acyl groups to facilitate hydrophobic interactions (Zhou and Troy 2005). Such a model raises the question: do polyprenols preferentially interact with certain lipid types? It has been reported that the effect of dolichol on the phase behavior of model membranes depends on the particular phospholipid with which it is co-dispersed (Wang et al. 2008). Intriguingly, other membrane-altering isoprenoids, such as cholesterol, exhibit strong partiality for lipids with specific degrees of saturation and defined head groups (Harroun et al. 2006). If indeed polyprenols have a preference for a particular lipid class, it may also influence their distribution between the outer and inner envelope membrane, which differ significantly in their lipid composition (Block et al. 1983; Douce and Joyard 1990).

It remains to be established how polyprenols reach their final membrane destination, following their synthesis in the stroma, and it is unclear if polyprenols accumulate into specific microdomains or are uniformly distributed throughout the envelope and thylakoid membranes. Nevertheless, the influence of polyprenols on chloroplast ultrastructure was evident, based on transmission electron micrograph images of polyprenol-deficient chloroplasts. In these plastids, a reduced stacking of thylakoid grana and increased numbers of plastoglobuli were consistently observed. This may indicate a general stress response brought about by polyprenol deficiency, however, as both of these plastid phenotypes can also be triggered by a variety of abiotic challenges (Musser et al. 1984; Hugly and Somervillle 1992; Cruz et al. 2001; Wang et al. 2014). Nonetheless, the effect that polyprenol abundance appears to have on plastidial ultrastructure and membrane integrity is striking considering that on a molar basis, plastidial polyprenols are a thousand times less abundant than their fatty acid co-residents (see fatty acid content in Fig. S4 versus plastidial polyprenol content in Fig. 5B assuming a ~2.12 µg/µL chlorophyll concentration). Taken together, these results lend support to the recently held notion that polyprenols act as 'superlipids' and that they may serve a more evolutionary conserved function than previously thought.

MATERIALS AND METHODS

Chemicals and Reagents

Polyclonal antibodies against Rbc-L, Tic40, and PsbA were obtained from Agrisera. Peptide-specific antibodies against SlCPT5 (N-RVKDGNIEPEDINC-C) were prepared by Cedarlane laboratories. TLC plates (RP18, Silica gel 200 micron, 20 cm x 20 cm) were obtained from Mandel Scientific. Authentic polyprenol standards were obtained from Indofine chemical company (heptaprenol C35), Avanti Polar Lipids (polyprenol mixture C65-C105), the Institute of Biochemistry and Biophysics Collection of Polyprenols (polyprenol mixture C45-C125), and Cedarlane Labs (GPP, NPP, FPP, GGPP). Radiolabeled 14C-IPP, 50.6 mCi (1.872 GBq

mmol-1, 0.02 mCi ml-1) was obtained from PerkinElmer. Macerozyme R-10 and Cellulase Onozuka R-10 were from Yakult. Synthetic drop-out media lacking histidine was obtained from US Biological. Standard molecular biology reagents (restriction enzymes, T4 DNA ligase, Taq-polymerases, etc.) were from Thermo-Scientific and all synthetic oligonucleotides were synthesized by Sigma-Aldrich and listed in Table S1). All other chemicals were obtained from Sigma-Aldrich or Thermo-Scientific.

Plant Material, Growth Conditions, and RNAi-mediated knockdown of SlCPT5

Wildtype and transgenic *Arabidopsis thaliana* (Col-0) and tomato (MP-1) plants were grown in potting soil (Sunshine Mix LA4) and maintained in a growth chamber under a 16hr photoperiod (150 µmol m-2 s-2; mixed cool white and incandescent bulbs). Arabidopsis was grown at 23ºC/18ºC and tomato at 26 ºC/18ºC (day/night). Relative humidity was maintained at 60%. For RNAi-mediated knockdown of SlCPT5, two fragments corresponding to base pairs 118-933 and 118-705 of the open reading frame were ligated in a sense/antisense orientation between the *Sac*I/*Eco*RI and *Bam*HI/*Eco*RI sites of the pSAT4A vector to obtain a hairpin construct under the control of the 35S promoter, enhancer, and terminator sequences (Tzfira et al. 2005). The hairpin cassette was transferred into the pPZP200 binary vector (Hajdukiewicz et al. 1994) and introduced into the MP-1 tomato cultivar by the University of Nebraska Plant Transformation Facility (https://biotech.unl.edu/plant-transformation) using established *Agrobacterium*-mediated plant transformation methods. Transgenic plants were selected on MS media supplemented with 100 µg L-1 kanamycin and the degree of SlCPT5 mRNA knockdown in ten independent transformants was assessed by quantitative RT-PCR as described below. The transgenic plants that were utilized for experimentation in this study were T4 homozygous lines.

RNA extraction and quantification

Total RNA was extracted from tomato leaf tissue using the RNeasy Plant Mini Kit (Qiagen) and the mRNA was reverse-transcribed to cDNA using the High Capacity cDNA Reverse Transcriptase Kit (Applied Biosystems). Quantitative RT-PCR analysis was performed in a Step One-Plus Real-Time PCR System (Applied Biosystems) using SYBR GREEN Master Mix (Quantabio) under the following cycling conditions: 95ºC for 10min, 40 cycles of 95ºC for 15sec and 52ºC for 1min. Each run was concluded with a melt curve analysis consisting of 95ºC for 15sec and 52ºC increasing to 95º by 0.3ºC per 1min. All reactions were performed in triplicate along with a no-template control. The relative expression levels of each target were determined according to the 2-ΔCt method (Livak and Schmittgen, 2001) and normalized against the tomato elongation factor 1α (EF1A; Solyc06g009970).

Polyisoprenoid and plastidial isoprenoid analysis

For polyisoprenoid analysis, approximately 3g of fresh tomato leaf tissue was frozen in liquid nitrogen and ground to a fine powder with a mortar and pestle. Lipids were extracted with a mixture of chloroform:methanol [1:1] containing 240 nM Pren-15 as an internal standard for 2h at 37ºC. Following phase separation, the non-polar extract was removed and the remaining tissue was re-extracted with chloroform:methanol [2:1]. The extracts were combined, evaporated under nitrogen and dissolved in a mixture containing 8% NaOH (from a 50 M stock solution), 50% toluene, and 42% ethanol (v/v/v) including 5 mM pyrogallol. Following hydrolysis for 1h at 95ºC, polyisoprenoids were extracted three times with hexane, applied to a silica gel 60 column and purified using isocratic elution with 15% diethyl ether in hexane, as described by Gawarecka and Swiezewska (2014). Polyisoprenoids within

chloroplasts and their various subcompartments were extracted as above except that hydrolysis was performed with 8% KOH (from a 17.8 M stock solution), 50% toluene and 42% ethanol (v/v/v) including 5 mM pyrogallol. Fractions containing polyisoprenoids were pooled, evaporated under nitrogen, and dissolved in 2-propanol. Yeast polyisoprenoids were extracted from 3 g of pelleted yeast cells with 10 mL of 25% KOH in 65% ethanol for 1h at 95 °C, and subsequently extracted and purified as described above. Polyisoprenoids were analyzed using an Agilent 1260 Infinity HPLC system equipped with a ZORBAX XDB-C18 reversed-phase column (4.6 × 75 mm, 3.5 µm, Agilent). Polyisoprenoids were eluted with a linear gradient from 0% to 100% methanol:isopropanol:hexane [2:1:1] in water:methanol [1:9] at a flow rate of 1.5 mL min-1. Polyisoprenoids were detected by absorbance at 210 nm and quantified relative to authentic standards. For the analysis of carotenoids, thylakoids and envelope fractions (prepared as described above) were extracted with a mixture of acetone:ethyl acetate:water [1.5:2:2]. The non-polar extract was analyzed by HPLC equipped with a Spherisorb ODS-2 reversed-phase column (250 × 4.6 mm, 5 µm, Supelco) according to the method of Norris et al. (1995). External calibration standards included β-carotene, lutein, neoxanthin, and violaxanthin. Tocopherols in the thylakoid and envelope fractions were extracted with a mixture of chloroform:methanol:water [2:2:1.8] supplemented with 7.5 µM Tocol as an internal standard. Following phase separation, the non-polar extract was dried under nitrogen, dissolved in hexane and analyzed by HPLC equipped with a LiChrosorb Si60A normal phase column (250 X 4.6 mm, 5 µm, Supelco), according to the method of Collakova and Dellapenna (2001, 2003).

Fatty acid analysis

Chloroplasts were isolated from tomato leaf tissue as outlined above (Salvi et al. 2011) and resuspended in 1ml of 25mM Tricine, pH 7.8, 330mM sorbitol, 5mM MgCl2, and 2.5mM EDTA. An aliquot (100µl) was removed for determining chlorophyll concentration and the remaining sample was centrifuged at 1500g for 5min at 4ºC and then resuspended in 900µl of 1N methanolic HCl containing 1mM pentadecanoic acid as the internal standard. Samples were heated for 2h at 85ºC and then cooled to room temperature prior to the addition of 900µl of a 0.9% NaCl solution and 270µl of hexane. Following gentle mixing and phase separation the non-polar extract was collected and analyzed by GC-MS (Agilent Technologies 78910A GC, 5975C inert MSD) equipped with a Bruker BR-WAX column (30m length, 0.25mm I.D., 0.50µm phase thickness). The carrier gas was helium, the inlet temperature was set at 240ºC and the injection was carried out in splitless mode. The GC oven was set to 50ºC for 1min and increased to 250ºC at 5ºC/min to be held at 250ºC for 10min. The MS transfer line was set to 260ºC with the source temperature at 230ºC. The data was acquired in electron impact (EI) positive ionization mode at 70eV energy and scan mode from 10amu to 300amu. Individual fatty acids methyl esters were identified by comparing their retention times to authentic standards (FAME Mix, C4-C24; Sigma).

Functional complementation of the yeast *Δrer2* mutant

The yeast *Δrer2* mutant strain YG932 (MATα *Δrer2*::kanMX4 ade2-101 ura3-52 his3-200 lys2-801) was cultured in yeast peptone dextrose (YPD) medium supplemented with 200 mg L-1 of G418 (Sato et al., 1999). The SlCPT5 and RER2 open-reading frames were PCR amplified and ligated between the *Sma*I and *Bam*HI restriction sites of the yeast expression vector pRS423 downstream of the native RER2 promoter sequence (Akhtar et al. 2013). These constructs along with the empty vector were introduced into the *Δrer2* mutant strain according to the method of Gietz and Schiestl (2007) and transformants were selected on

synthetic drop-out media without histidine supplemented with G418, 0.67% yeast nitrogen base and 2% glucose. For *in vivo* complementation assays, the individual transformants were grown in YPD media supplemented with 200 mg L-1 of G418 to an OD600 of 1.0 and 3µl was streaked out onto duplicate plates which were incubated at 25°C and 37°C, respectively.

SlCPT5 purification and enzyme activity

The open reading frame of *SlCPT5* was amplified by PCR beginning at Ser-43 to exclude the predicted transit peptide, inserted into the pEXP-5-CT/TOPO vector system (Invitrogen), and then introduced into *E. coli* BL21-CodonPlus (DE3)-RIPL cells. Bacterial cells expressing recombinant SlCPT5 were cultured in LB media at 37°C to an OD600 of 0.6 at which point isopropyl-β-D-thiogalactoside was added to a final concentration of 1 mM and then incubated at 16°C for an additional 20 hours. *E. coli* cells were harvested by centrifugation, resuspended in lysis buffer (20 mM Tris, pH 8.0, 500 mM KCl), and then disrupted with an EmulsiFlex-C3 (Avestin). Crude protein extracts were clarified by centrifugation at 12,000 x g for 10 min at 4°C and then applied to a 1 mL HisTrap HP column (GE Healthcare) equilibrated in lysis buffer and affixed to an AKTA Pure FPLC system (GE Healthcare). The Ni2+ affinity matrix was washed with five column volumes of lysis buffer containing 20 mM imidazole and the remaining bound proteins were eluted with one column volume of lysis buffer containing 400 mM imidazole and immediately desalted on PD-10 gel filtration columns (GE Healthcare) equilibrated with 50 mM HEPES, pH 8.0, 100 mM KCl, 7.5 mM MgCl2, 5 mM DTT, 0.1% Triton X-100, and 10% (v/v) glycerol. Assays for determining SlCPT5 enzyme activity were performed using ~1 µg of purified SlCPT5 recombinant protein in a 50µL reaction volume containing 20 µM of *trans*-prenyl diphosphate (GPP, NPP, FPP, or GGPP) acceptor substrate and 14C-IPP (50 mCi mmol-1) at a final concentration of 40 µM (100 nCi). The enzymatic products were dephosphorylated by acid hydrolysis (0.6 M HCl, 30 min at 37°C), extracted with three volumes of ethyl acetate and quantified by scintillation counting. The remaining extracts were applied to a 60 Å silica gel TLC plate, developed with acetone:water (39:1) and visualized by autoradiography and compared to the retardation factor (*Rf*) value of co-chromatographed authentic polyprenol standards (C35-C125) that were stained with iodine vapor to determine the size of the enzymatic products. SlCPT5 kinetic parameters were determined by non-linear regression analysis using the Michaelis-Menten kinetics model of the SigmaPlot 12.3 software and CPT activity in chloroplast subcompartments was determined according to the methods described by Akhtar et al. (2017).

Homology modeling and site-directed mutagenesis

For molecular modeling and *in silico* docking studies, the protein sequence of mature SlCPT5 lacking its chloroplast targeting peptide was modeled with SWISS-MODEL (Arnold et al., 2006; Biasini et al., 2014; Bordoli et al., 2008) using the crystal structure of lavandulyl diphosphate synthase from *L. x intermedia* as the template (Liu et al. 2016) and visualized using the PyMOL Molecular Graphics System, version 1.3 (Schrödinger, LLC). The quality of the model was assessed using PROCHECK (Laskowski et al., 1993) and ERRAT(Colovos and Yeates, 1993). Mutagenesis of SlCPT5 was performed using the QuikChange II Site-Directed Mutagenesis Kit (Agilent) with the pEXP-CT-TOPO/SlCPT5 expression vector (see above) as a template. Mutagenic primers (supplemental table 1) were designed to produce the following amino acid changes in SlCPT5: D89A, F133A, R259S, and R265S. These mutated variants of SlCPT5 were ligated between the *Sma*I and *Bam*HI of the pRS423 vector

and then introduced into the yeast *Δrer2* mutant, as described above. For complementation assays, the various yeast strains (beginning with a culture of cells at an OD600 of 0.5) were serially diluted on agar plates containing synthetic drop-out media without histidine (supplemented with G418) and incubated at 23°C and 37°C, as described above.

Subcellular localization and chloroplast fractionation

The open-reading frame of SlCPT5 was amplified by PCR and ligated between the *Xho*I and *Bam*HI sites of the pSAT6A vector which creates an in-frame C-terminal fusion protein with GFP (Falara et al. 2010). This construct was mobilized into protoplasts that were prepared from *Arabidopsis thaliana* (Col-0) rosette leaves via 'tape-sandwich' method (Wu et al., 2009). Fluorescence attributed to GFP (500-530 nm) and chlorophyll autofluorescence (650-700 nm) were visualized with a Leica SP5 confocal laser scanning microscope equipped with a 488 nm argon laser for fluorophore excitation. Immunolocalization of SlCPT5 was performed on chloroplast subcompartments (envelope, stroma, and thylakoids) that were prepared according to the method of Salvi et al. (2011) from ~20g of tomato leaf tissue using a leaf grinding buffer composed of 50 mM Tris-HCl, pH 8.0, 350 mM sorbitol, 5 mM EDTA, 0.1% (w/v) BSA, and 15 mM β-mercaptoethanol. Crude protein extracts from chloroplasts, envelope, stroma and thylakoid fractions were resolved by SDS-PAGE and immunoblotted with peptide-specific antibodies raised against SlCPT5 or with the compartment-specific antibodies to assess the purity of each subfraction. For measurements of photosynthetic electron transport and differential scanning calorimetry assays (see below), thylakoid membranes were isolated from ~1g of tomato leaf tissue according to Method II described by Chen et al. (2016).

Photosynthetic electron transport and CO2 assimilation measurements

Linear photosynthetic electron transport rates were measured according to the method of Dean and Miskiewicz (2003) with thylakoids that were isolated as described above. Briefly, isolated thylakoids (30µg of chlorophyll) were mixed with 8mL of Hill Reaction Buffer (25mM Tris-HCl, pH 7.4 containing100 mM sorbitol, 10 mM NaCl, and 5 mM NH4Cl) and 2,6-dichlorophenolindophenol (DCPIP) was added to a final concentration of 30 µM. The DCPIPlabeled thylakoids were then transferred into 1mL cuvettes, covered with parafilm to prevent reoxidation of DCPIP, and then illuminated with 20 µmol m-2 sec-1 of photosynthetically active radiation generated by a desktop lamp. Samples were scanned spectrophotometrically at 600nm every 2 minutes for 14 minutes to determine the rate of DCPIP reduction. For CO2 assimilation measurements, fully expanded young leaves (~2.5 weeks old) were excised from wild type or the RNAi lines and placed into a sealed chamber under a light emitting diode and CO2 (400 parts per million, balanced in air) was pumped into the chamber at a rate of ~200 mL/min. The photosynthetically active photon flux density (PPFD) was adjusted from 100 to 1000 µmol m-2 s-2 and the concentration of CO2 gas leaving the chamber was analyzed with an infrared gas analyzer after passing through a humidity/temperature sensor and a drying column (containing drierite). Leaves were analyzed under eight different PPFDs (100, 200, 300, 400, 500, 600, 800 and 1000 µmol m-2 s-2) for 5 min each at 25ºC. CO2 assimilation rates were calculated as the change in CO2 concentration (ΔCO2) over the total leaf area per second using a Q-S151 CO2 analyzer (Quibit Systems) equipped with the Logger Pro software package.

Fluorescence anisotropy measurements

The relative fluidity of plastidial envelope membranes was determined by measuring the steady-state fluorescence polarization (anisotropy, *r*) of membranes that were embedded with the lipophilic fluorophore, 1,6-diphenyl-1,3,5-hexatriene (DPH). Envelope membranes were isolated as described above, except that MgCl2 was omitted from all buffers used in the isolation procedure. Membranes (0.1 mg mL-1 protein) were then incubated with 5 µM DPH in the dark at room temperature for 40 min and subsequently brought to a final concentration of 20 µg mL-1 protein and 1 µM DPH in DPH fluorescence buffer (25mM Tricine, pH 7.8 containing 100mM sorbitol and 10 mM NaCl). Anisotropy measurements were obtained by exciting DPH-labelled membranes with vertically polarized light at a wavelength of 360 nm and detecting emitted polarized light at 460 nm using a Photon Technology International model 814 spectrofluorometer system. The degree of fluorescent polarization was calculated according to the following equation:

$$r = lVV - GlVH \,/\, lVV + 2GlVH$$

where *I*vv and *I*vh represent the components of emitted fluorescence that are polarized parallel and perpendicular to the plane of the polarized excitation beam with the first and second subscript representing the position of the excitation and emission polarizers (vertical and horizontal, respectively). The *G* factor ($G = lHV\ lHH$) is a correction coefficient that compensates for any unequal transmission optics of the system and was determined by scanning 1 µM of DPH in fluorescence buffer (Ameloot et al. 2013). To account for light scattering, the fluorimeter was blanked prior to scans with samples of unlabeled envelope membranes in DPH fluorescent buffer.

Chloroplast ultrastructure

Fully-expanded leaves (2.5 weeks old) were selected from wild type and the independent RNAi lines to analyze chloroplast ultrastructure. Tissue was excised in 0.2 M phosphate buffer with 5% gluteraldehyde [v/v] and fixed overnight in modified Karnovsky's fixative solution (Karnovsky 1965) containing 2% formaldehyde, 2.5% glutaraldehyde and 0.1 M sodium phosphate buffer, pH 7.2. Samples were washed three times in a 0.1 M phosphate buffer and then fixed again overnight in 0.1 M phosphate buffer with 1% OsO4 [v/v] . After three washes with deionized water, samples were sequentially dehydrated with ethanol (50%, 70%, 90% and 95%) deionized water [v/v]) for 30 min each. The dehydrated samples were washed twice in 100% ethanol followed by two washes in propylene oxide for 2 hr each. Samples were then incubated in a series of Spurr resin gradients (2:1, 1:1 and 1:2 propylene oxide: Spurr resin) for 2 hr each and then washed twice in 100% Spurr resin for 1 hr. Samples were then placed in an embedding mold (Polysciences Inc., USA) with Spurr resin and baked at 70ºC for at least 8 hr. Sections (100 nm) were sectioned with an ultramicrotome (Leica Ultracut UCT) and mounted onto formvar and carbon coated 100 mesh copper TEM grids. Sections were stained with 2% uranyl acetate and Reynolds' lead citrate (Reynold 1963). Images were obtained with a transmission electron microscope (FEI Tecnai F20 G2) with a Gatan 4K bottom mounted camera.

Differential Scanning Calorimetry

Measurements of thylakoid membrane integrity were determined using a TA Instruments Q2000 differential scanning calorimeter. Thylakoids were prepared as described above, diluted to a chlorophyll concentration of 2 mg mL-1,and 10 µL of the solution was transferred into hermetic aluminum alodine pans (TA Instruments). Samples were heated from 20 to

100°C at a ramping rate of 1°C min-1. After the initial ramp, samples were immediately cooled to 20°C, and then heated again (as described above) to examine the reversibility of the thermal transitions. The transition temperature (*T*m) was defined as the peak of the excess heat capacity curve, and the enthalpy required for the thermal unfolding and denaturation of thylakoid membrane proteins (Δ*H*) was determined from the area under the curve.

FUNDING INFORMATION
This work was supported by grants from the National Science Centre of Poland [UMO-2016/21/B/NZ1/02793] to L. Surmacz, from the Ontario Ministry of Agriculture, Food and Rural Affairs (OMAFRA) to T.A. Akhtar and from the Natural Sciences and Engineering Research Council of Canada (NSERC) to T. A. Akhtar.

DISCLOSURES
Conflicts of interest: No conflicts of interest declared

ACKNOWLEDGMENTS
We thank Tannis Slimmon and Michael Mucci (University of Guelph) for help with plant growth maintenance. We are grateful to Dr. Steffen Graether and Dr. Janet Wood (University of Guelph) for advice with fluorescence anisotropy measurements, and thank Michaela Strüder-Kypke and Robert Harris (University of Guelph) for technical advice on confocal and electron microscopy. Lastly, we thank Drs. Fernanda Peyronel and Alejandro G. Marangoni (University of Guelph) for their technical expertise and guidance with differential scanning calorimetry analysis.

REFERENCES
Akhtar, T.A., Matsuba, Y., Schauvinhold, I., Yu, G., Lees, H.A., Klein, S.E., et al. (2013) The tomato cis-prenyltransferase gene family. *Plant J.* 73: 640-652.

Akhtar, T.A., Surowiecki, P., Siekierska, H., Kania, M., Van Gelder, K., Rea, K.A., et al. (2017) Polyprenols are synthesized by a plastidial cis-prenyltransferase and influence photosynthetic performance. *Plant Cell* 29: 1709-1725.

Albright, C.F., Orlean, P. and Robbins, P.W. (1989) A 13-amino acid peptide in three yeast glycosyltransferases may be involved in dolichol recognition. *Proc. Natl. Acad. Sci. USA* 86: 7366-7369.

Ameloot, M., vandeVen, M., Acuňa, A.U. and Valeur, B. (2013) Fluorescence anisotropy measurements in solution: methods and reference materials (IUPAC technical report). *Pure Appl. Chem.* 85: 589-608.

Arnold, K., Bordoli, L., Kopp, J. and Schwede, T. (2006) The SWISS-MODEL workspace: a web-based environment for protein structure homology modelling. *Bioinformatics* 22: 195-201.

Bajda, A., Konopka-Postupolska, D., Krzymowska, M., Hennig, J., Skorupinska-Tudek, K., Surmacz, L., et al. (2009) Role of polyisoprenoids in tobacco resistance against biotic stresses. *Physiol. Plantarum* 135: 351–364.

Biasini, M., Bienert, S., Waterhouse, A., Arnold, K., Studer, G., Schmidt, T., et al. (2014) SWISS-MODEL: modelling protein tertiary and quaternary structure using evolutionary information. *Nucleic Acids Res.* 42: W252–W258.

Block, M.A., Dorne, A.J., Joyard, J. and Douce, R. (1983) Preparation and characterization of membrane fractions enriched in outer and inner envelope membranes from spinach chloroplasts. II. Biochemical characterization. *J. Biol. Chem.* 258: 13281-13286

Bordoli, L., Kiefer, F., Arnold, K., Benkert, P., Battey, J. and Schwede, T. (2008) Protein structure homology modeling using SWISS-MODEL workspace. *Nat. Protoc.* 4: 1–13.

Brasher, M.I., Surmacz, L., Leong, B., Pitcher, J., Swiezewsk, E., Pichersky, E., et al. (2015) A two-component enzyme complex is required for dolichol biosynthesis in tomato. *Plant J*. 82: 903–914.

Chang, S.Y., Ko, T.P., Liang, P.H. and Wang, A.H.J. (2003) Catalytic mechanism revealed by the crystal structure of undecaprenyl pyrophosphate synthase in complex with sulfate, magnesium, and Triton. *J. Biol. Chem.* 278: 29298–29307.

Chen, Y.E., Yuan, S. and Schröder, W.P. (2016) Comparison of methods for extracting thylakoid membranes of Arabidopsis plants. *Physiol. Plant* 156: 3-12.

Chojnacki, T. and Vogtman, T. (1984) The occurrence and seasonal distribution of C50-C60 polyprenols and of C100- and similar long-chain polyprenols in leaves of plants. *Acta. Biochim. Pol.* 31: 115-126.

Collakova, E. and DellaPenna, D. (2001) Isolation and functional analysis of homogentisate phytyltransferase from Synechocystis sp. PCC 6803 and Arabidopsis. *Plant Physiol.* 127: 1113-1124.

Collakova, E. and DellaPenna, D. (2003) Homogentisate phytyltransferase activity is limiting for tocopherol biosynthesis in Arabidopsis. *Plant Physiol*. 131: 632–642.

Colovos, C. and Yeates, T.O. (1993) Verification of protein structures: Patterns of nonbonded atomic interactions. *Protein Sci.* 2: 1511–1519.

Cruz, J.A., Salbilla, B.A., Kanazawa, A. and Kramer, D.M. (2001) Inhibition of plastocyanin to P700 + electron transfer in Chlamydomonas reinhardtii by hyperosomtic stress. *Plant Phsyiol.* 127: 1167-1179.

Daleo, G.R. and Lezica, R.P. (1977) Synthesis of dolichol phosphate by a cell-free extract from pea. *FEBS Lett.* 74: 247-250.

Datta, A.K. and Lehrman, M.A. (1993) Both potential dolichol recognition sequences of hamster GlcNAc-1-phosphate transferase are necessary for normal enzyme function. *J. Bio. Chem.* 268: 12663-12668.

Dean, R.L. and Miskiewicz, E. (2003) Rates of electron transport in the thylakoid membranes of isolated, illuminated chloroplasts are enhanced in the presence of ammonium chloride. *Biochem. Mol. Biol. Edu.* 31: 410-417.

Dobrikova, A.G., Busheva, M.C., Taneva, S.G. and Petkanchin, I.B. (1997) Electric dipole moments of PS I-enriched membrane fragments. *J. Photoch. Photobio. B* 39: 30-35.

Dobrikova, A.G., Várkonyi, Z., Krumova, S.B., Kovács, L., Kostov, G.K., Todinova, S.J., et al. (2003) Structural rearrangements in chloroplast thylakoid membranes revealed by differential

scanning calorimetry and circular dichroism spectroscopy. Thermo-optic effect. *Biochemistry* 42: 11272-11280.

Douce, R. and Joyard, J. (1990) Biochemistry and function of the plastid envelope. *Annu. Rev. Cell Biol.* 6: 173–216.

Falara, V., Akhtar, T.A., Nguyen, T.T.H., Spyropoulou, E.A., Bleeker, P.M., Schauvinhold, I., et al. (2011) The tomato terpene synthase gene family. *Plant Physiol.* 157: 770-789.

Fei, Z., Joung, J.G., Tang, X., Zheng, Y., Huang, M., Lee, J.M., et al. (2011) Tomato functional genomics database: a comprehensive resource and analysis package for tomato functional genomics. *Nucleic Acids Res.* 39: 1156-1163.

Ford, R.C. and Barber, J. (1983) Incorporation of sterol into chloroplast thylakoid membranes and its effect on fluidity and function. *Planta* 158: 35–41.

Fujihashi, M., Zhang, Y.W., Higuchi, Y., Li, X.Y., Koyama, T. and Miki, K. (2001) Crystal structure of cis-prenyl chain elongating enzyme, undecaprenyl diphosphate synthase. *Proc. Natl. Acad. Sci. USA* 98: 4337–4342.

Gawarecka, K. and Swiezewska, E. (2014) Analysis of plant polyisoprenoids. *Method Mol. Biol.* 1153: 135-147.

Gietz, R.D. and Schiestl, R.H. (2007) High-efficiency yeast transformation using the LiAc/SS carrier DNA/PEG method. *Nat. Protoc.* 2: 31–34.

Govindjee, J.J.S. and van Rensen, J.J.S. (1978) Bicarbonate effects on the electron flow in isolated broken chloroplasts. *Biochim. Biophys. Acta* 505: 183–213.

Gruszecki, W.I. and Strzałka, K. (2005) Carotenoids as modulators of lipid membrane physical properties. *Biochim. Biophys. Acta* 1740: 108-115.

Guo, R.T., Ko, T.P., Chen, A.P.C., Kuo, C.J., Wang, A.H.J. and Liang, P.H. (2005) Crystal structures of undecaprenyl pyrophosphate synthase in complex with magnesium, isopentenyl pyrophosphate, and farnesyl thiopyrophosphate: roles of the metal ion and conserved residues in catalysis. *J. Biol. Chem.* 280: 20762–20774.

Hajdukiewicz, P., Svab, Z. and Maliga, P. (1994) The small, versatile pPZP family of Agrobacterium binary vectors for plant transformation. *Plant Mol. Biol.* 25: 989–994.

Handa, N., Terada, T., Doi-Katayama, Y., Hirota, H., Tame, J.R.H., Park, S.Y., et al. (2005) Crystal structure of a novel polyisoprenoid-binding protein from Thermus thermophilus HB8. *Protein Sci.* 14: 1004-1010.

Harroun, T.A., Katsaras, J. and Wassall, S.R. (2006) Cholesterol hydroxyl group is found to reside in the center of a polyunsaturated lipid membrane. *Biochemistry* 45: 1227-1233.

Hartley, M.D. and Imperiali, B. (2012) At the membrane frontier: A prospectus on the remarkable evolutionary conservation of polyprenols and polyprenyl-phosphates. *Arch. Biochem. Biophys.* 517: 83–97.

Hasan, S.S. and Cramer, W.A. (2012) On rate limitations of electron transfer in the photosynthetic cytochrome *b6f* complex. *Phys. Chem. Chem. Phys.* 14: 13853-13860.

Havaux, M. (1998) Carotenoids as membrane stabilizers in chloroplasts. *Trends Plant Sci.* 3: 147-151.

Heber, U., Neimanis, S. and Dietz, K.J. (1988) Fractional control of photosynthesis by the QB protein, the cytochrome f/b 6 complex and other components of the photosynthesic apparatus. *Planta* 173: 267–274.

Hemming, F.W. (1983) The biosynthesis of polyisoprenoid chains. *Biochem. Soc. T.* 11: 497-503.

Hugly, S., Kunst, L., Browse, J. and Somerville, C. (1989) Enhanced thermal tolerance of photosynthesis and altered chloroplast ultrastructure in a mutant of Arabidopsis deficient in lipid desaturation. *Plant Physiol.* 90: 1134-1142.

Hugly, S. and Somerville, C. (1992) A role for membrane lipid polyunsaturation in chloroplast biogenesis at low temperature. *Plant Phsyiol.* 99: 197-202.

Karnovsky, M.J. (1965) A formaldehyde-glutaraldehyde fixative of high osmolality for use in electron microscopy. *J. Cell Biol.* 27: 137-138.

Kera, K., Takahashi, S., Sutoh, T., Koyama, T. and Nakayama, T. (2012) Identification and characterization of a cis,trans-mixed heptaprenyl diphosphate synthase from Arabidopsis thaliana. *FEBS J.* 279: 3813–3827.

Kharel, Y., Takahashi, S., Yamashita, S. and Koyama, T. (2006) Manipulation of prenyl chain length determination mechanism of cis-prenyltransferases. *FEBS J*. 273: 647-657.

Kharel, Y., Zhang, Y.W., Fujihashi, M., Miki, K. and Koyama, T. (2001) Identification of significant residues for homoallylic substrate binding of Micrococcus luteus B-P 26 undecaprenyl diphosphate synthase. *J. Biol. Chem.* 276: 28459–28464.

Kirby, J. and Keasling, J.D. (2009) Biosynthesis of plant isoprenoids: perspectives for microbial engineering. *Annu. Rev. Plant Biol.* 60: 335–355.

Kirchhoff, H., Haferkamp, S., Allen, J.F., Epstein, D.B. and Mullineaux, C.W. (2008) Protein diffusion and macromolecular crowding in thylakoid membranes. *Plant Physiol.* 146: 1571-1578.

Krumova, S.B., Laptenok, S.P., Kovács, L., Tóth, T., Van Hoek, A., Garab, G., et al. (2010)Digalactosyl-diacylglycerol-deficiency lowers the thermal stability of thylakoid membranes. *Photosynth Res.* 105: 229-242.

Kunst, L., Browse, J. and Somerville, C. (1989) Enhanced thermal tolerance in a mutant of Arabidopsis deficient in palmitic acid unsaturation. *Plant Physiol.* 91: 401-408.

Kurisaki, A., Sagami, H. and Ogura, K. (1997) Distribution of polyprenols and dolichols in soybean plant. *Phytochemistry* 44: 45–50.

Laczkó-Dobos, H., Todinova, S., Sözer, Ö., Komenda, J., Kis, M., Sallai, A., et al. (2011) Identification of thylakoid membrane thermal transitions in Synechocystis sp. PCC6803 photosynthetic mutants. *Photosynth Res.* 107: 237-246.

Laskowski, R.A., MacArthur, M.W., Moss, D.S. and Thornton, J.M. (1993) PROCHECK: a program to check the stereochemical quality of protein structures. *J. Appl. Crystallogr.* 26: 283-291.

Lentz, B.R. (1993) Use of fluorescent probes to monitor molecular order and motions within liposome bilayers. *Chem. Phys. Lipids* 64: 99–116.

Liang, P.H. (2009) Reaction kinetics, catalytic mechanisms, conformational changes, and inhibitor design for prenyltransferases. *Biochemistry* 48: 6562–6570.

Lindgren, B.O. (1965) Homologous aliphatic C30-C45 terpenols in birch wood. *Acta Chem. Scand.* 19: 1317–1326.

Livak, K.J. and Schmittgen, T.D. (2001) Analysis of relative gene expression data using realtime quantitative PCR and the 2(-Delta Delta C(T)) method. *Methods* 25: 402-408.

Liu, M., Chen, C.C., Chen, L., Xiao, X., Zheng, Y., Huang, J.W., et al. (2016) Structure and function of a “head-to-middle” prenyltransferase: lavandulyl diphosphate synthase. *Angew. Chem. Int. Ed. Engl.* 55: 4721-4724.

Matsuba, Y., Zi, J., Jones, A.D., Peters, R.J. and Pichersky, E. (2015) Biosynthesis of the diterpenoid lycosantalonol via nerylneryl diphosphate in Solanum lycopersicum. *PLoS One* 10: e0119302.

McCloskey, M.A. and Troy, F.A. (1980) Paramagnetic isoprenoid carrier lipids. 2. Dispersion and dynamics in lipid membranes. *Biochemistry* 19: 2061-2066.

McCourt, P., Kunst, L., Browse, J. and Somerville, C.R. (1987) The effects of reduced amounts of lipid unsaturation on chloroplast ultrastructure and photosynthesis in a mutant of Arabidopsis. *Plant Physiol.* 84: 353-360.

Musser, R.L., Thomas, S.A., Wise, R.R., Peeler, T.C. and Naylor, A.W. (1984) Chloroplast ultrastructure, chlorophyll fluorescence, and pigment composition in chilling-stressed soybeans. *Plant Physiol.* 74: 749-754.

Norris, S.R., Barrette, T.R. and DellaPenna, D. (1995) Genetic dissection of carotenoid synthesis in Arabidopsis defines plastoquinone as an essential component of phytoene desaturation. *Plant Cell* 7: 2139-2149.

Pogson, B., McDonald, K.A., Truong, M., Britton, G. and DellaPenna, D. (1996) Arabidopsis carotenoid mutants demonstrate that lutein is not essential for photosynthesis in higher plants. *Plant Cell* 8: 1627-1639.

Popova, A.V. and Hincha, D.K. (2007) Effects of cholesterol on dry bilayers: interactions between phosphatidylcholine unsaturation and glycolipid or free sugar. *Biophys. J.* 93: 1204-1214.

Ravi, K., Rip, J. and Carroll, K. (1984) Differences in polyisoprenoid alcohols of mono-and dicotyledonous seeds. *Lipids* 19: 401-404.

Reynolds, E.S. (1963) The use of lead citrate at high pH as an electron-opaque stain in electron microscopy. *J. Cell Biol.* 17: 208-212.

Rodríguez-Concepción, M. and Boronat, A. (2002) Elucidation of the methylerythritol phosphate pathway for isoprenoid biosynthesis in bacteria and plastids. A metabolic milestone achieved through genomics. *Plant Physiol.* 130: 1079–1089.

Rohmer, M. (1999) The discovery of a mevalonate-independent pathway for isoprenoid biosynthesis in bacteria, algae and higher plants. *Nat. Prod. Rep.* 16: 565–574.

Rush, J.S., Matveev, S., Guan, Z., Raetz, C.R. and Waechter, C.J. (2010) Expression of functional bacterial undecaprenyl pyrophosphate synthase in the yeast rer2Δ mutant and CHO cells. *Glycobiology* 20: 1585–1593.

Sakaihara, T., Honda, A., Tateyama, S. and Sagami, H. (2000) Subcellular fractionation of polyprenyl diphosphate synthase activities responsible for the syntheses of polyprenols and dolichols in spinach leaves. *J. Biochem.* 128: 1073–1078.

Salvi, D., Moyet, L., Seigneurin-Berny, D., Ferro, M., Joyard, J. and Rolland, N. (2011) Preparation of envelope membrane fractions from Arabidopsis chloroplasts for proteomic analysis and other studies. *Method Mol. Biol.* 775: 189–206.

Sato, M., Sato, K., Nishikawa, S., Hirata, A., Kato, J. and Nakano, A. (1999) The yeast RER2 gene, identified by endoplasmic reticulum protein localization mutations, encodes cisprenyltransferase, a key enzyme in dolichol synthesis. *Mol. Cell Biol.* 19: 471–483.

Schilmiller, A.L., Schauvinhold, I., Larson, M., Xu, R., Charbonneau, A.L., Schmidt, A., et al. (2009) Monoterpenes in the glandular trichomes of tomato are synthesized from a neryl diphosphate precursor rather than geranyl diphosphate. *Proc. Natl. Acad. Sci. USA* 106: 10865-10870.

Schulbach, M.C., Brennan, P.J. and Crick, D.C. (2000) Identification of a short (C15) chain Zisoprenyl diphosphate synthase and a homologous long (C50) chain isoprenyl diphosphate synthase in Mycobacterium tuberculosis. *J. Biol. Chem.* 275: 22876-22881.

Shinitzky, M. and Barenholz, Y. (1978) Fluidity parameters of lipid regions determined by fluorescence polarization. *BBA–Rev. Biomembranes* 515: 367-394.

Skorupinska-Tudek, K., Poznanski, J., Wojcik, J., Bienkowski, T., Szostkiewicz, I., Zelman-Femiak, M., et al. (2008) Contribution of the mevalonate and methylerythritol phosphate pathways to the biosynthesis of dolichols in plants. *J. Biol. Chem.* 283: 21024-21035.

Smith, K.A. and Low, P.S. (1989) Identification and partial characterization of the denaturation transition of the light harvesting complex II of spinach chloroplast membranes. *Plant Phsyiol.* 90: 492-499.

Surmacz, L. and Swiezewska, E. (2011) Polyisoprenoids: Secondary metabolites or physiologically important superlipids? *Biochem. Bioph. Res. Co.* 407: 627–632.

Swiezewska, E. and Chojnacki, T. (1988) Long-chain polyprenols in gymnosperm plants. *Acta Biochim. Pol.* 35: 131-147.

Swiezewska, E. and Danikiewicz, W. (2005) Polyisoprenoids: structure, biosynthesis and function. *Prog. Lipid Res.* 44: 235–258.

Swiezewska, E., Sasak, W., Mańkowski, T., Jankowski, W., Vogtman, T., Krajewska, I., et al. (1994) The search for plant polyprenols. *Acta Biochim. Pol.* 41: 221–260.

Tholl, D. and Lee, S. (2011) Terpene specialized metabolism in Arabidopsis thaliana. *Arabidopsis* Book 9: e0143.

Tzfira, T., Tian, G.W., Lacroix, B., Vyas, S., Li, J., Leitner-Dagan, Y., et al. (2005) pSAT vectors: a modular series of plasmids for autofluorescent protein tagging and expression of multiple genes in plants. *Plant Mol. Biol.* 57: 503–516.

Wang, X., Mansourian, A.R. and Quinn, P.J. (2008) The effect of dolichol on the structure and phase behavior of phospholipid model membranes. *Mol. Membr. Biol.* 25: 547-556.

Wang, S., Uddin, M.I., Tanaka, K., Yin, L., Shi, Z., Qi, Y., et al. (2014) Maintenance of chloroplast structure and function by overexpression of the rice monogalactosyldiacylglycerol synthase gene leads to enhanced salt tolerance in tobacco. *Plant Physiol.* 165: 1144-1155.

Wu, F.H., Shen, S.C., Lee, L.Y., Lee, S.H., Chan, M.T. and Lin, C.S. (2009) Tape-Arabidopsis Sandwich - a simpler Arabidopsis protoplast isolation method. *Plant Methods* 5: 16.

Yamamoto, Y., Ford, R.C. and Barber, J. (1981) Relationship between thylakoid membrane fluidity and the functioning of pea chloroplasts: effects of cholesteryl hemisuccinate. *Plant Physiol.* 67: 1069–1072.

Yang, Z. and Brouillette, C.G. (2016) A guide to differential scanning calorimetry of membrane and soluble proteins in detergents. *Methods Enzymol.* 567: 319-358.

Zhou, G.P. and Troy II, F.A. (2003) Characterization by NMR and molecular modeling of the binding of polyisoprenols and polyisoprenyl recognition sequence peptides: 3D structure of the complexes reveals sites of specific interactions. *Glycobiology* 13: 51–71.

Zhou, G.P. and Troy II, F.A. (2005) NMR studies on how the binding complex of polyisoprenol recognition sequence peptides and polyisoprenols can modulate membrane structure. *Curr. Protein Pept. Sci.* 6: 399–411.

Table I. Kinetic parameters of SlCPT5 with NPP, GPP, FPP or GGPP as substrates

Substrate	K_m (μM)	K_{cat} (s^{-1})	K_{cat}/K_m (s^{-1} M^{-1})
NPP	29.82 ± 6.80	0.106 ± 0.007	3.55×10^3
GPP	13.00 ± 5.15	0.040 ± 0.004	3.08×10^3
FPP	4.85 ± 0.84	0.119 ± 0.004	2.45×10^4
GGPP	3.48 ± 0.96	0.079 ± 0.004	2.27×10^4

Measurements were made at room temperature in 50 mM HEPES buffer, pH 8.0, containing, 5 mM DTT, 7.5 mM MgCl2, 100 mM KCl, 10% (v/v) glycerol, 0.1% (v/v) Triton-X-100. Reactions were started by adding 14C-IPP substrate. Data are the means of three independent determinations ± SE.

Table II. Tocopherol and carotenoid content in wild-type and RNAi thylakoid and envelope membranes.

	Thylakoids (µg mg Chl^{-1})		Envelope (µg mg $protein^{-1}$)	
	WT	RNAi	WT	RNAi
Carotenoids	100.61 ± 2.72	95.58 ± 9.19	6.79 ± 2.71	6.86 ± 0.32
Tocopherols	1.95 ± 0.681	1.87 ± 0.779	4.63 ± 2.11	8.27 ± 2.06

Thylakoid and envelope membranes were obtained via sucrose gradient fractionation according to Salvi et al. (2011). From these isolated membranes carotenoids and tocopherols were separately extracted, purified and analyzed via reverse and normal-phase (respectively) highperformance liquid chromatography following the methods outlined by Pogson et al. (1996), Norris et al. (1995) and Collakova and DellaPenna (2001; 2003). Data are the means of at least three independent replicates, ± SE.

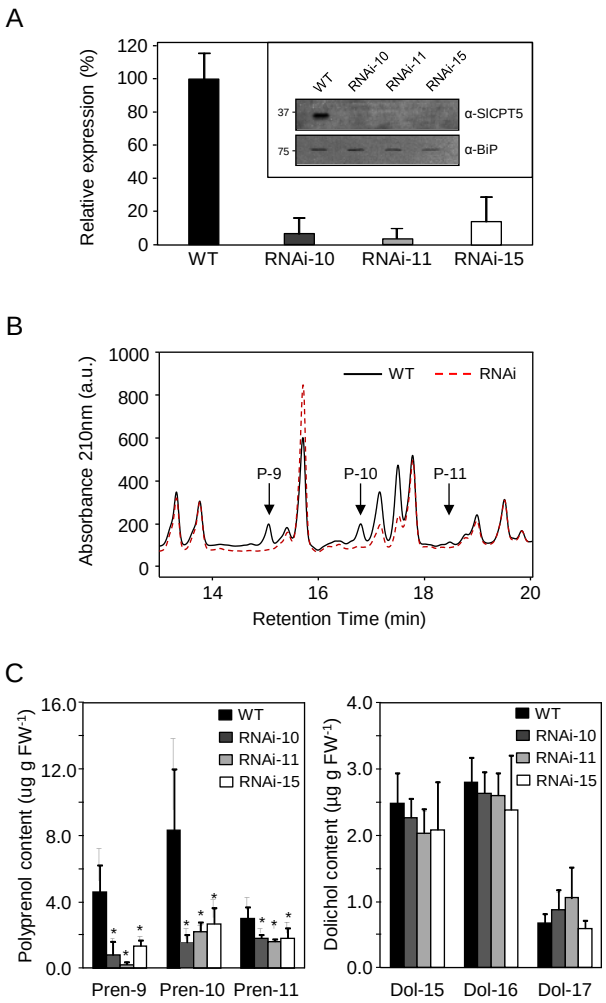

Figure 1. RNAi-mediated knockdown of SlCPT5. A, SlCPT5 gene expression in tomato leaves from wildtype (WT) and in three independent RNAi lines (RNAi-10, 11 and 15). Data are the mean expression values ± SD from three biological replicates and are presented as a percentage of wildtype SlCPT5 gene expression. Crude leaf extracts from these plants were probed for SlCPT5 protein expression via immunoblot analysis using a peptide-specific antibody against SlCPT5; the expression of BiP in these immunoblots was monitored simultaneously to ensure for equal sample loading and the size of each target protein in kDa is indicated by the molecular weight markers (*inset*). B, Total leaf polyisoprenoid analysis; a representative HPLC/UV chromatogram of a polyisoprenoid extract from the leaves of wildtype (solid line) versus RNAi (red dotted line) lines is shown. The presence of the main polyprenols (P-9, P-10, and P-11) found in each sample are indicated. C, Quantification of leaf polyprenols (Pren-9 to Pren-11) and dolichols (Dol-15 to Dol-17) in wildtype and RNAi lines. Data are the means ± standard deviation from at least five independent extractions. Asterisks indicate a significant difference ($P < 0.05$) in polyprenol content when compared to those found in wild type leaves.

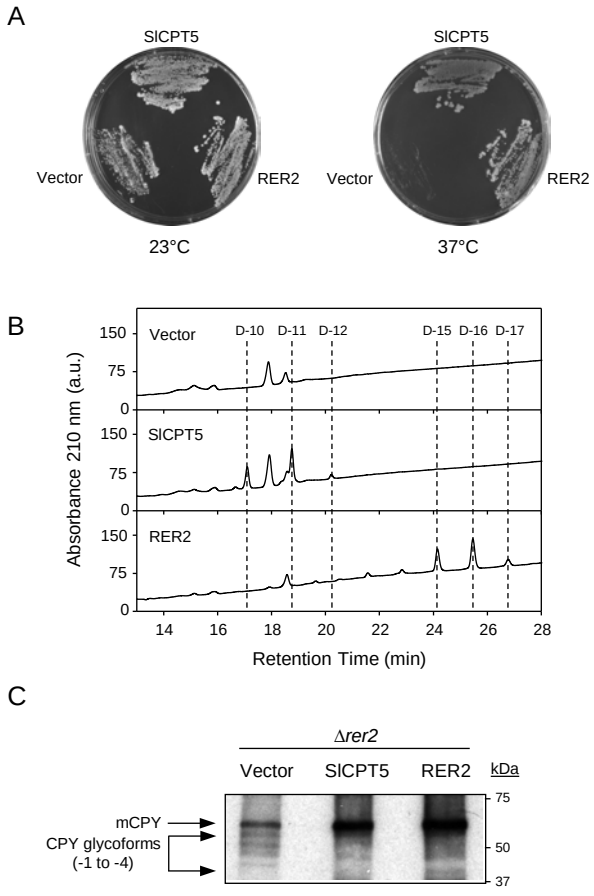

Figure 2. Functional complementation of the dolichol-deficient yeast mutant (*rer2*Δ) by SlCPT5. A, The SlCPT5 open reading minus the predicted *N*-terminal transit peptide was introduced into the yeast *rer2*Δ mutant under control of the native RER2 promoter and transformed cells were grown at the indicated temperatures. As positive and negative controls the mutant was also transformed with the native RER2 gene and the expression vector alone, respectively. B, Polyisoprenoid content in yeast cells from the indicated strains were analyzed for dolichols. Note the accumulation of medium chain dolichols (D-10 to D-12) in the *rer2*Δ mutant cells containing SlCPT5 and longer chain dolichols (D-15 to D-17) in mutant cells containing the native RER2 gene. C, Restoration of carboxypeptidase Y (CPY) glycosylation status by SlCPT5. Soluble crude protein extracts from the various *rer2*Δ strains were subjected to immunoblot analysis using antibodies specific for CPY. The positions and molecular weight (kDa) of mature CPY (mCPY) and its hypoglycosylated forms missing between one and four (-1 to -4) *N*-linked oligosaccharides are indicated.

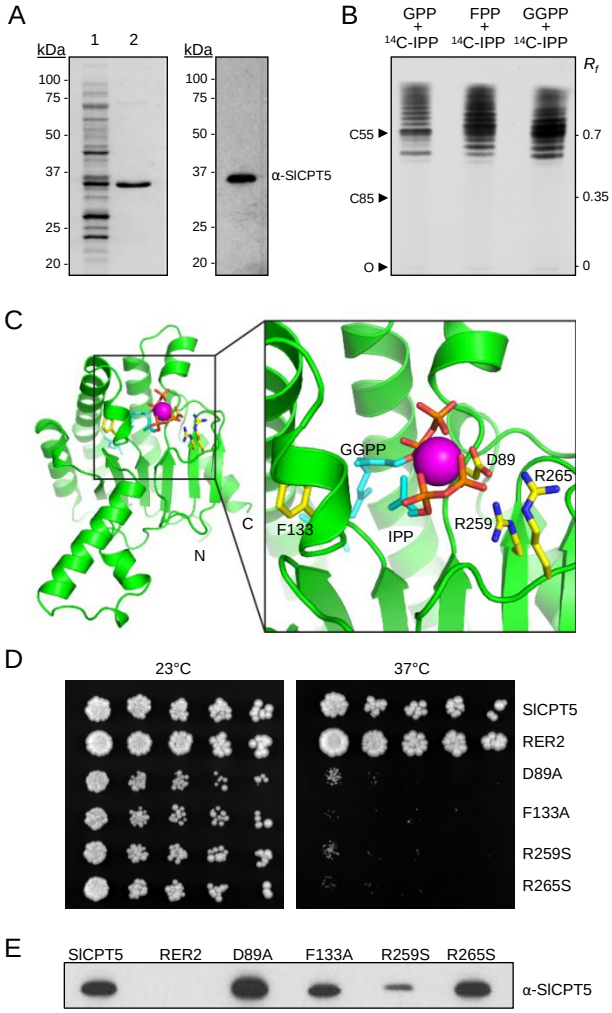

Figure 3. Enzyme characterization of SlCPT5. A, Purification of SlCPT5 by Ni^{2+}-affinity chromatography. Proteins were separated by SDS-PAGE and stained with Coomassie Blue. Lanes 1 and 2 contain *E. coli* extract and purified protein, respectively. Adjacent to this is an immunoblot of the purified protein using a peptide specific antibody for SlCPT5 (α-SlCPT5). B, Analysis of enzymatic reaction products. De-phosphorylated reaction products were resolved on reverse-phase silica gel plates and developed by autoradiography. The position of C55, the major product, was determined based on the retardation factor (R_f) of authentic polyprenol standards of known size (C10-C120). C, Homology modeling of SlCPT5 to the lavandulyl diphosphate synthase from *Lavandula x. intermedia* (LiLPPS; PDB ID: 5hc6). The position of residues important for substrate coordination and catalysis, previously identified in bacteria, are shown in yellow with nitrogens coloured blue and oxygens coloured red. Magnesium is shown as a purple sphere and GGPP and IPP are shown as cyan sticks and labeled. D, Complementation of the *rer2Δ* yeast mutant by SlCPT5. Serial dilutions of *rer2Δ* yeast cells expressing the native RER2, SlCPT5 or various mutants of SlCPT5 were plated at the indicated temperatures. E, Immunoblot analysis of SlCPT5 protein levels in the various mutant yeast strains. Crude protein extracts were obtained from each yeast strain described above and probed for SlCPT5 abundance.

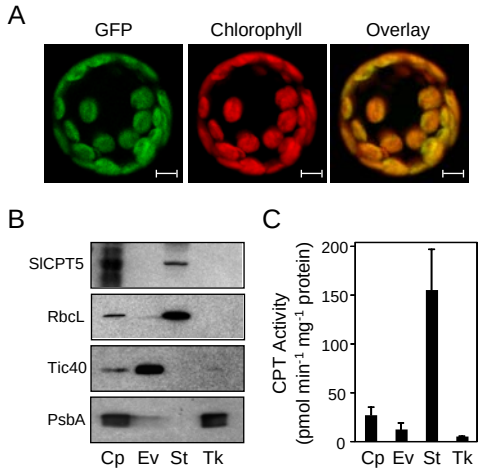

Figure 4. Subcellular localization of SlCPT5. A, Arabidopsis protoplasts transiently expressing SlCPT5 fused at the C-terminus to GFP. Fluorescence attributable to GFP, chlorophyll and their merged signals were observed by confocal microscopy. Bars = 5µm. B, Fractionation of chloroplasts from wild type tomato leaves. Intact chloroplasts (Cp) were fractioned into envelope (Ev), stroma (St), and thylakoid (Tk) compartments by sucrose gradient centrifugation. Protein samples from each fraction were analyzed by immunoblotting using antibodies specific for SlCPT5, the Rubisco large subunit (RbcL), the Tic40 component of the inner envelope translocon, or the D1 reaction center protein (psbA) of photosystem II. C, CPT enzyme activity in chloroplasts. Intact chloroplasts from tomato leaf tissue were fractioned as above and each compartment was assayed for CPT enzyme activity using GGPP and ^{14}C-IPP as substrates. Data represent the means ± SD from four independent experiments.

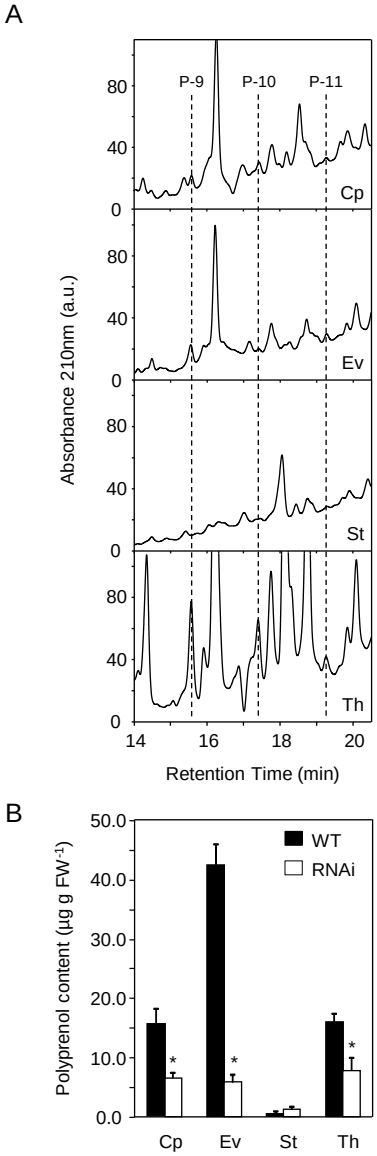

Figure 5. The distribution of plastidial polyprenols. A, Representative HPLC chromatograms illustrating the main polyprenols (P-9, P-10, and P-11) that are present in the chloroplasts (Cp) and their various subcompartments (envelope, Ev; stroma, St; and thylakoids, Th) from wild type tomato leaves. B, Quantification of plastidial polyprenols. The abundance of polyprenols in the various chloroplast subcompartments from the leaves of wild type and the SlCPT5 RNAi lines is shown. Data are the means ± SE from at least four independent preparations of each plastidial fraction and asterisks indicate a significant difference (*P<0.05*) in polyprenol content when compared to wildtype levels.

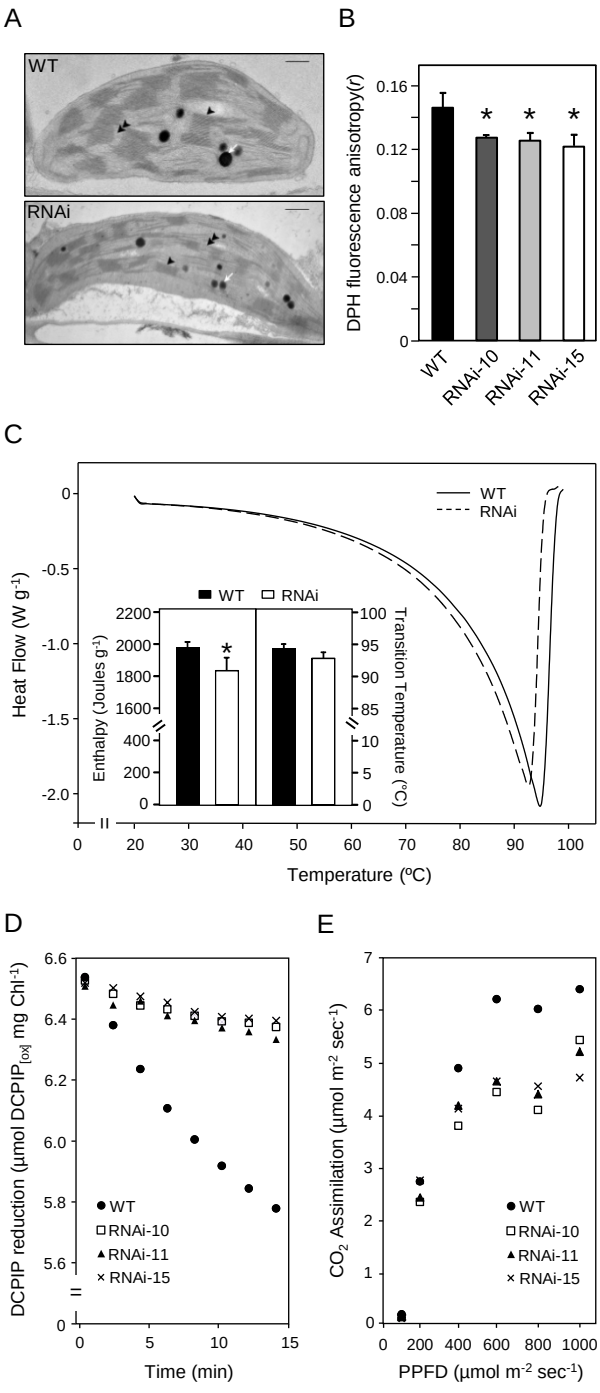
A
WT
RNAi
B
DPH fluorescence anisotropy(r)
0.16
0.12
0.08
0.04
0
*
*
*
WT
RNAi-10
RNAi-11
RNAi-15
C
Heat Flow (W g-1)
0
-0.5
-1.0
-1.5
-2.0
WT
RNAi
Enthalpy (Joules g-1)
2200
2000
1800
1600
400
200
0
Transition Temperature (°C)
100
95
90
85
10
5
0
0
20
30
40
50
60
70
80
90
100
Temperature (ºC)
D
DCPIP reduction (µmol DCPIP[ox] mg Chl-1)
6.6
6.4
6.2
6.0
5.8
5.6
0
WT
RNAi-10
RNAi-11
RNAi-15
0
5
10
15
Time (min)
E
CO2 Assimilation (µmol m-2 sec-1)
7
6
5
4
3
2
1
0
WT
RNAi-10
RNAi-11
RNAi-15
0
200
400
600
800
1000
PPFD (µmol m-2 sec-1)

Figure 6. The effects polyprenol deficiency on plastidial membrane dynamics and photosynthetic performance. A, Changes in chloroplast ultrastructure. Representative transmission electron micrographs of mesophyll chloroplasts from the leaves of wild type (*upper panel*) and the SlCPT5 RNAi lines (*lower panel*). Note the increased number of plastoglobuli and the diminished grana stacking in chloroplasts from the RNAi lines. Arrow – plastoglobuli; arrow head – thylakoid grana; double arrow head – stromal thylakoids. Scale bar = 0.5 µm. B, Envelope membrane fluidity. Plastidial envelope membranes prepared from wild type and the three independent SlCPT5 RNAi lines were labeled with 1,6-diphenyl-1,3,5-hexatriene (DPH) and the degree of steady state DPH fluorescence polarization was determined by fluorescence anisotropy measurements. Data are the means ± standard error from four independent envelope preparations from each plant line; asterisks indicate significant difference (Student's *t* test, $P < 0.05$) when comparing *r* values to those obtained from wild type samples. C, Changes in thylakoid protein stability. Representative thermograms from thylakoids prepared from wild type and the RNAi lines were obtained by differential scanning calorimetry (DSC) over the indicated temperature range. Note the shift towards lower transition temperatures and calorimetric enthalpies associated with thylakoids isolated from the RNAi lines (*inset*). Data are the means ± SE from at least five independent preparations of thylakoids from each plant line described above and asterisks indicate a significant difference ($P < 0.05$) when comparing values to wild type. D, Photosynthetic electron transport rates. Thylakoids were isolated from wild type and the RNAi lines and then illuminated in the presence of oxidized 2,6-dichlorophenolindophenol (DCPIP) over the indicated timespan. The rate of DCPIP reduction was measured spectrophotometrically by scanning samples at 600nm every 2 minutes. E, Light response curves of CO_2 assimilation rates. Detached leaves from wild type and the SlCPT5 RNAi lines were exposed to increasing PPFD and CO_2 assimilation rates were calculated as the change in CO_2 concentration over the total leaf area per second. Data from D and E represent the mean values obtained from at least five independent preparations of thylakoids (D) or individual detached leaves (E) from each of the indicated plant lines.